NASA TECHNICAL NOTE

NASA TN D-3622

NASA TN D-3622

PREDICTION OF THE INVERSION LOAD OF A CIRCULAR TUBE

by LeRoy R. Guist and Donald P. Marble

Ames Research Center
Moffett Field, Calif.

NATIONAL AERONAUTICS AND SPACE ADMINISTRATION • WASHINGTON, D. C. • SEPTEMBER 1966

NASA TN D-3622

PREDICTION OF THE INVERSION LOAD OF A CIRCULAR TUBE

By LeRoy R. Guist and Donald P. Marble

Ames Research Center
Moffett Field, Calif.

NATIONAL AERONAUTICS AND SPACE ADMINISTRATION

For sale by the Clearinghouse for Federal Scientific and Technical Information
Springfield, Virginia 22151 – Price $1.00

PREDICTION OF THE INVERSION LOAD OF A CIRCULAR TUBE

By LeRoy R. Guist and Donald P. Marble
Ames Research Center

SUMMARY

This study is concerned with the plastic deformation process encountered in the inversion or turning inside out of a circular tube. The load required to cause inversion is derived analytically from elementary expressions for plastic energy absorbed during uniaxial plastic straining. Analytical results are compared with the results of experiments conducted concurrently, and with previously reported results. Experimental values of inversion load agreed with analytical predictions within 10 to 30 percent.

INTRODUCTION

Interest in the "inversion tube" arose from consideration of energy absorbing devices suitable for use in the landing structure of space vehicles. A discussion of some of the other concepts being considered for soft landings of space vehicles is presented in reference 1. The use of an inversion tube to absorb energy is suggested in reference 2 and applications of the inversion tube in a lunar landing system are discussed in reference 3.

The inversion process involves the turning inside out of a tube acted upon by a compressive load. Experimental results indicate that the process is feasible only for certain very ductile materials and only for a certain range of tube thickness to diameter ratios. The inversion process is shown schematically in figure 1, for both inside-out and outside-in configurations. Experimental results indicate that the process occurs at constant load, and the final diameter has an equilibrium value depending upon initial diameter and thickness.

The primary purpose of this study was to predict analytically the axial load required to cause inversion, and to provide sufficient experimental data to test the validity of the analysis. Secondary purposes were to study dynamic properties and consider some design variations. Only the inside-out configuration is discussed in this report.

SYMBOLS

A cross-sectional area of tube wall

c curvature parameter defined in figure 3

D original mean diameter of tube

D_i mean diameter of tube after inversion

e plastic strain

L total length of tube

P inversion load

t thickness of tube

U total plastic strain energy absorbed

V volume of material plastically deformed

x travel of inversion load

x_A length of tube experiencing plastic deformation

ρ material density

σ_p perfectly plastic yield stress

ANALYSIS

The analytical model is a circular cylinder of thickness t in which each increment of length experiences plastic bending and hoop extension while passing from its original diameter D through a half toroidal shape to its final diameter D_i (fig. 2). It is assumed that the original tube assumes curvature suddenly at A, has a constant curvature through the toroidal region while expanding in the hoop direction, and then straightens suddenly at B. Both the curvature of the bending process and the amount of hoop extension are expressed as functions of the curvature parameter c. The following assumptions have been made in this analysis.

1. The material is perfectly plastic and the effect of biaxial stresses on the yield stress is neglected.

2. The work done by the inversion load is entirely dissipated as internal plastic work in the three processes mentioned above.

3. Both thickness changes and changes in axial length are ignored. (Corrections for these effects are discussed under experimental results.)

4. The inversion process is completely independent of axial travel x, occurring at constant inner and outer diameter. It is assumed that the outer diameter seeks an equilibrium value determined by the curvature parameter c.

5. The inversion process occurs at constant load.

The load required to cause inversion was derived by two methods: (1) equating the incremental work done by the inversion load to the incremental plastic energy absorbed, and (2) summing forces and moments on an elemental radial segment of the toroidal portion of the model. The resulting expressions for inversion load were identical, but the work method will be presented because of its greater simplicity.

Derivation of Inversion Load From Plastic Strain Energy Absorbed

The plastic energy U absorbed while the inversion load P has moved a distance x (fig. 3) is

$$U = Px \tag{1}$$

In view of the analytical model defined earlier, it is clear that U consists of energy absorbed in three separate processes: bending at A, extension from A to B, and bending at B. It is assumed that the bending processes at A and B are identical, hence, the combined bending energy is simply twice the energy absorbed in bending at A. The plastic work is expressed as the product of plastic stress σ_p, the average strain e, and the volume of material deformed, $V = Ax_A$,

$$U = A\sigma_p(2e_B + e_E)x_A \tag{2}$$

where e_B and e_E are the average bending and extensional strains, respectively, and x_A is the length of material inverted.

The plastic extensional strain e_E which occurs in the hoop direction is expressed as the change in circumference divided by the original circumference. From figure 3

$$\left.\begin{aligned} e_E &= \frac{\pi D_i - \pi D}{\pi D} = \frac{D_i - D}{D} \qquad \frac{D + 2ct - D}{D} \\ e_E &= 2c\,\frac{t}{D} \end{aligned}\right\} \tag{3}$$

where c is the curvature parameter defined in figure 3.

The expression for average plastic bending strain involves the assumption of a linear variation of strain across the tube thickness, which implies an average strain exactly half of the extreme fiber strain. The outer fiber strain from figure 3 is

$$e_{B_{max}} = \frac{[(c + 1)t/2] - (ct/2)}{ct/2} = \frac{1}{c}$$

hence,

$$e_B = 1/2c \tag{4}$$

Combining equations (2), (3), and (4):

$$U = A\sigma_p\left(\frac{1}{c} + 2c\,\frac{t}{D}\right)x_A \tag{5}$$

It is apparent from figure 2 that under equilibrium conditions, $x_A = (1/2)x$; hence, equation (5) becomes

$$U = \frac{A\sigma_p}{2}\left(\frac{1}{c} + \frac{2ct}{D}\right)x \tag{6}$$

and from equation (1):

$$P = \frac{A\sigma_p}{2}\left(\frac{1}{c} + \frac{2ct}{D}\right) \tag{7}$$

Equation (6) is not a purely analytical expression since it contains the parameter c which is not defined in terms of model parameters. Equation (7), however, indicates that the plastic energy absorbed in bending is inversely proportional to c while the extensional energy absorbed is proportional to c. Hence, the function in parentheses has a minimum value with respect to c and it is reasonable to hypothesize that the process will occur at this minimum value. The derivative of equation (6) with respect to c is zero at the minimizing value of c

$$c_m = \sqrt{\frac{D}{2t}} \tag{8}$$

Combining equations (7) and (8) yields

$$P = \pi Dt\sigma_p\sqrt{\frac{2t}{D}} = 4.44\ \sigma_p t^{3/2}D^{1/2} \tag{9}$$

which is a simple and useful expression for inversion load in terms of model parameters alone.

A measure of the energy absorbing capacity of the inversion tube is given by specific energy absorption (SEA) which is the energy absorbed divided by the weight of the specimen. A specimen of length L absorbs an amount of energy PL as the load moves a distance L, and the specimen weight is $\rho V = \rho AL$; hence, from equation (9),

$$SEA = \frac{\sqrt{2}\pi\sigma_p t^2\sqrt{(D/t)}L}{\rho(\pi Dt)L} = \frac{\sigma_p}{\rho}\sqrt{\frac{2t}{D}} \tag{10}$$

COMPARISON OF ANALYTICAL AND EXPERIMENTAL RESULTS

The tests conducted at Ames Research Center were intended to substantiate and extend the work reported in reference 2. Ames testing extended the range of values of t/D, considered larger scale specimens, investigated the effects of loading rate, and considered specimens with tapering wall thickness. Secondary testing included determining material stress-strain properties and a special test simulating only the bending process involved in inversion.

Equilibrium Value of c

A comparison of experimental values of the curvature parameter c and the minimum value given by equation (8) is shown in figure 4. The predicted value is seen to be greater than the experimental value by a factor of nearly 2. However, examination of equation (6) indicates that the term in parentheses is a very weak function of c with the result that a large discrepancy in c has a small effect on predicted inversion load. Hence, even though the analytical model is not adequate to predict the equilibrium value of c accurately, it provides a useful expression for the inversion load.

The change in thickness and length of inversion specimens was determined by measurements before and after inversion. It was found that the percentage thickness decrease was approximately equal to the percentage length decrease. Furthermore, the percentage change in either case was approximately half the hoop strain, thus satisfying the condition that material volume must remain constant. Since these two changes have opposing effects upon inversion load, it is felt that assuming constant thickness and length is a reasonable approximation.

Inversion Load

Figures 5 and 6 and table I compare analytical and experimental values of inversion load plotted against t. Figure 5 compares inversion load data from Ames tests of 1-inch diameter tubing with analytical values while figure 6 similarly compares data from reference 2. Table I compares predicted load with data from Ames tests of 2-inch and 8-inch diameter specimens. In these comparisons, two methods of predicting inversion load were used. In one, the purely analytical value obtained from equation (9) was used, and in the other, equation (7) was used with the experimental value of c given in figure 4. It is seen that the purely analytical prediction is in error by 20 to 30 percent while the prediction using the experimental value of c is in error by 10 to 20 percent. No explanation could be found to account for this discrepancy, although it is suspected that it is due to an effective higher yield point than the simple tensile yield point assumed in the analysis. The value of yield stress σ_p used in figures 5 and 6 and table I was obtained from a best fit of a perfectly plastic stress-strain diagram to the experimental stress-strain plot for the material used in the specimens. Figure 7 shows stress-strain curves for both 3003-H14 and 3003-H112 aluminum and the perfectly plastic diagrams used to idealize them. All aluminum specimens considered in this report with the exception of the 8-inch diameter ones (which were H112) were of 3003-H14 alloy. It is important to note the mechanism whereby the 3003-H14 alloy attains strains as high as 60 percent while the curve shown in

figure 7 indicates approximately 4-percent strain to failure. This apparent discrepancy can be resolved by noting that the curves of figure 7 indicate average strain over a 2-inch gage length while the strains occurring during inversion are comparable to those in the necked-down portion of a tensile specimen. To demonstrate this, the broken line in figure 7 was taken from measurements of stretching "within the neck" of the same specimen used for the solid curve. Since even these values are averages over some small length, the actual strains attained during inversion could be even higher. In the case of the 3003-H14 alloy, however, the material never reaches the "necking down" stress since this alloy is in the nearly annealed condition.

Inversion of Flat Strips

Special tests simulating only the bending process involved in inversion were made as shown in figure 8 with flat strips of 3003-H14 aluminum. The purpose of these tests was to determine the accuracy of the first term in the parentheses of equation (7) as a function of c. The spacing of the outer legs of the fixture was altered to simulate different values of c. Force measurements from these tests are plotted in figure 8 superimposed upon the curve representing the bending component of force given by equation (7). Comparison of these curves indicates good agreement for higher values of c but increasing error toward lower values. This might be expected since the effect of combined stresses ignored in the bending model becomes more important as bending strain levels increase. It is felt that the results given in figure 8 provide evidence that the analytical model is adequate for engineering predictions of inversion load.

Effect of Loading Speed

During the course of testing inversion specimens, it was noted that the inversion load increased with deformation speed even at relatively low speeds. Tests were performed at speeds from 10^{-5} to 30 ft/sec to define this variation. The range from 10^{-5} to approximately 1.0 ft/sec was investigated by means of a high-speed, closed-loop, hydraulic test machine while the range from 7.5 to 30 ft/sec was studied in drop tests. Results are shown in figure 9 for 3003-H14 aluminum tubes with 2-inch o.d. and 1/16-inch wall. These results indicate an increase of as high as 15 percent above static loads in the speed range tested. It is felt that higher speed tests would be exceedingly difficult to interpret, in terms of model properties, because of the transient dynamic behavior of the specimen at impact.

Tapered Inversion Specimen

In an effort to devise an energy absorber with a "softening" force deformation curve and a more failure proof design, the inversion specimen whose thickness diminished along its length was devised. As seen in figure 10, such a specimen is less likely to fail than a uniform tube since tensile stresses are carried in sections which are always thicker than the section being

deformed plastically. The force deformation curve is, as expected, softening in that inverting force decreases with increasing deflection, thereby decreasing the tendency for elastic rebound.

Energy Absorbing Efficiency

The specific energy absorption of the inversion tube is shown in figure 11 for the predicted inversion load as a function of t/D given by equation (10). This curve indicates that greater efficiencies are achieved as thickness increases and axial stress approaches the compressive yield stress of the tube.

CONCLUDING REMARKS

Analytical predictions of the inversion load of 3003-H14 specimens agree with test data within 20 to 30 percent and within 10 to 20 percent when the experimental value of the parameter c is used in the prediction. Predicted values of the curvature parameter c are greater than experimental values by a factor of nearly 2, but in view of the fact that energy absorbed and inversion load are weak functions of c, this discrepancy is not felt to be of great significance. An increase in inversion load of 15 percent above the "static" value of inversion load was obtained for deformation speeds as high as 30 ft/sec. The analysis is considered adequate for engineering predictions of inversion load of 3003-H14 tubes. Additional experimental work would be required to determine the accuracy of this prediction for tubes of other materials.

Ames Research Center
National Aeronautics and Space Administration
Moffett Field, Calif., June 16, 1966
124-08-04-02

REFERENCES

1. Esgar, Jack B.: Survey of Energy-Absorption Devices for Soft Landing of Space Vehicles. NASA TN D-1308, 1962.

2. Kroell, C. K.: A Simple, Efficient, One-Shot Energy Absorber. Shock, Vibration and Associated Environments, Part III, Bulletin 30. 30th Symposium on Shock, Vibration, and Associated Environments, Detroit, Mich., Oct. 10-12, 1961. Office of the Assistant Secretary of Defense. Jan. 1962.

3. Burns, A. B.; and Plascyk, J. A.: Lunar Alightment Systems Investigation. ASD-TR-63-454, June 1963. American Machine and Foundry Co., Stamford, Conn.

TABLE I.- INVERSION LOAD OF 2-INCH O.D. AND 8-1/2-INCH O.D. ALUMINUM TUBES

Diameter	Inversion load, lb, and percent error				
	Experimental	Equation (9)		Equation (7) with C from figure 4	
2-inch o.d.	2,650	2,060	22 percent	2,380	10.4 percent
8-1/2-inch o.d.	35,000	27,900	20 percent	31,000	11.4 percent

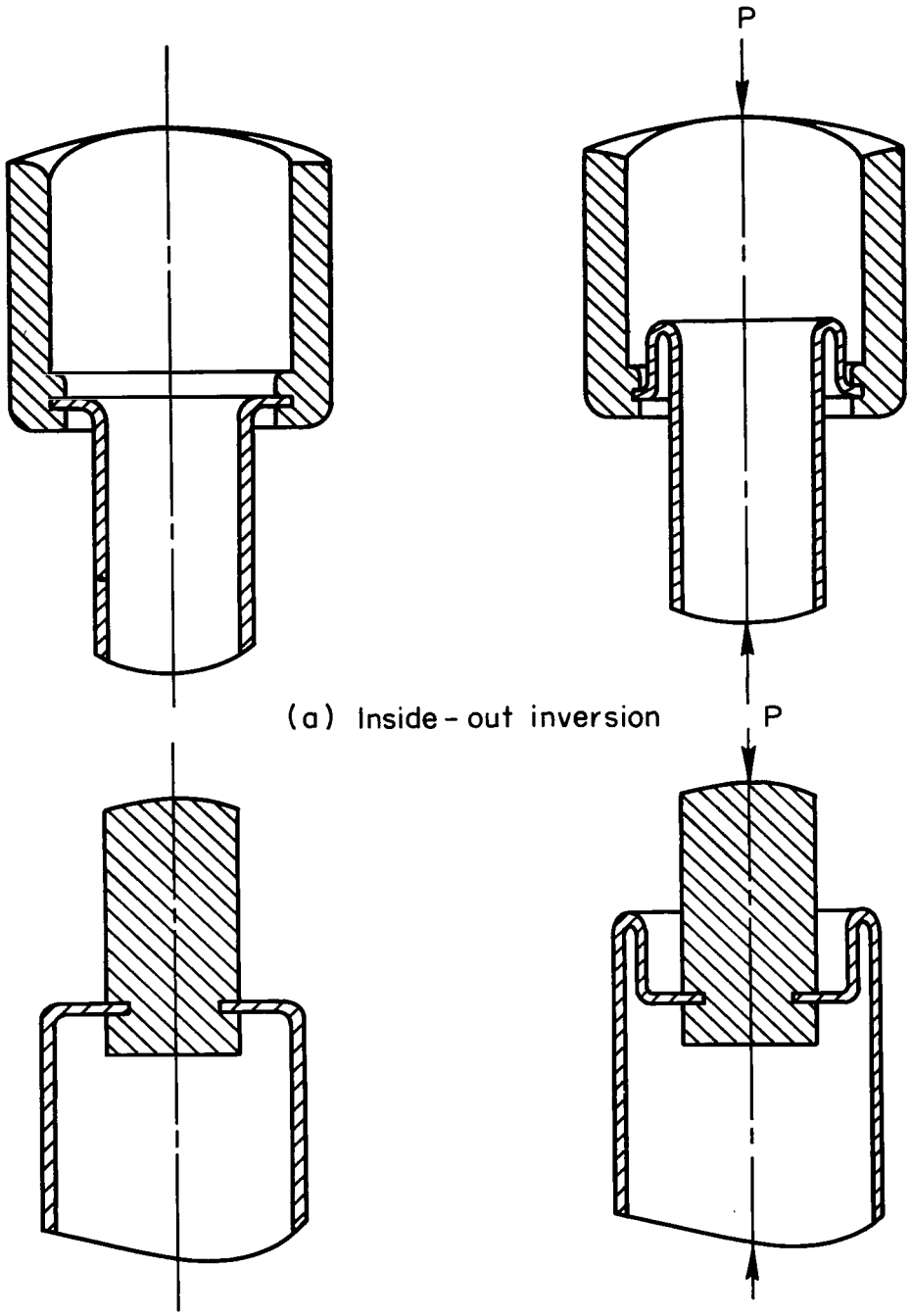

(a) Inside - out inversion

(b) Outside - in inversion

Figure 1.- Inversion of aluminum tube.

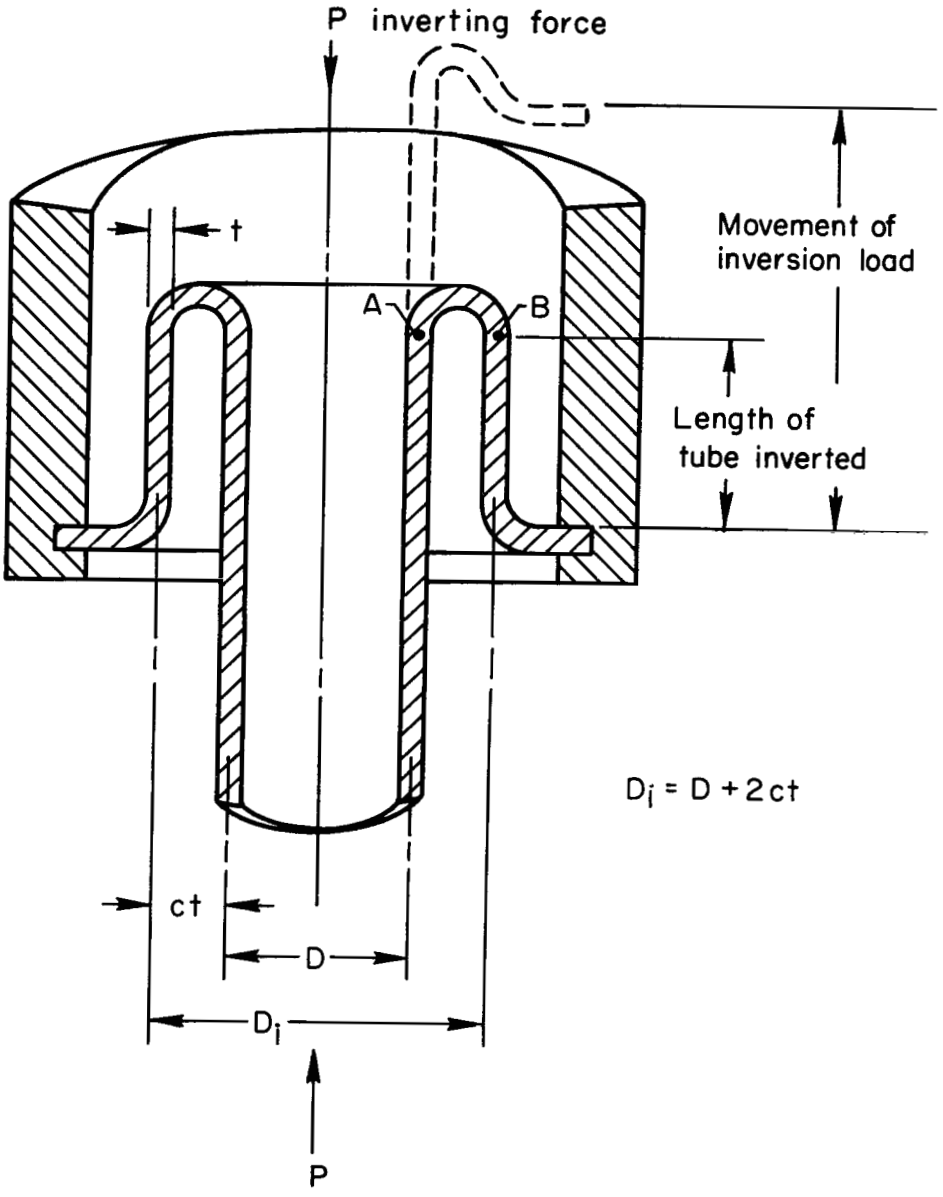

Figure 2.- Inverting process.

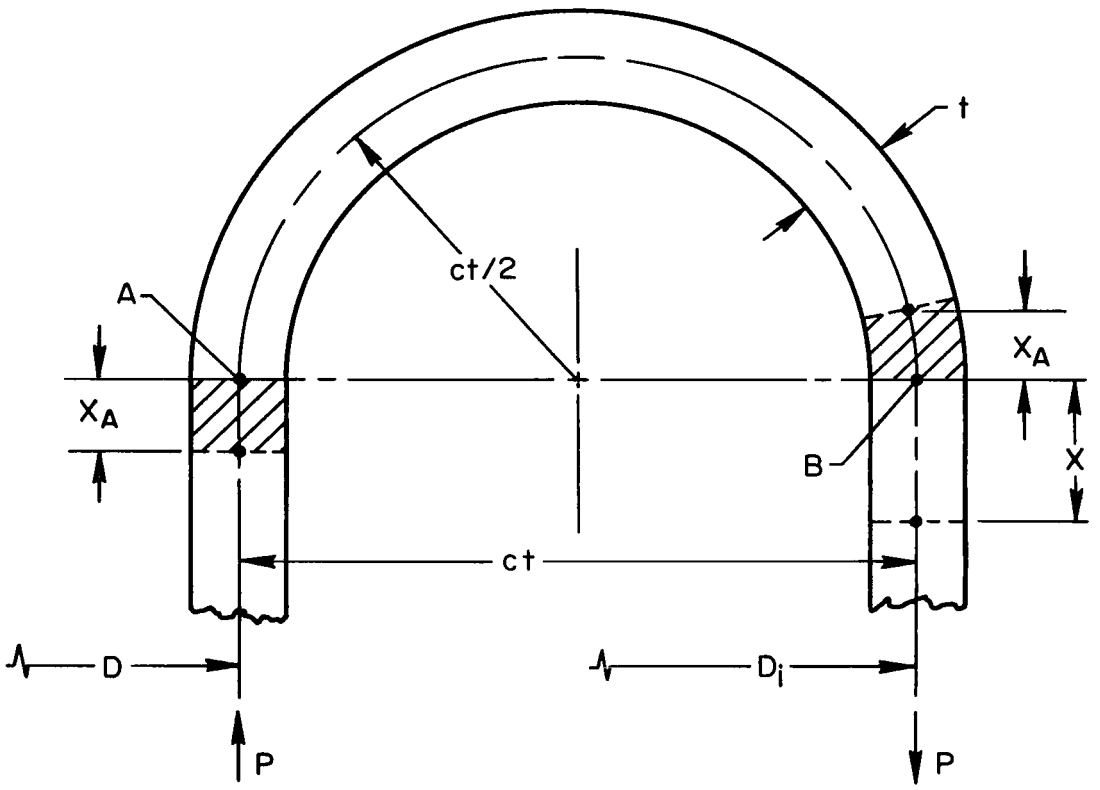

Figure 3.- Geometry of toroidal region.

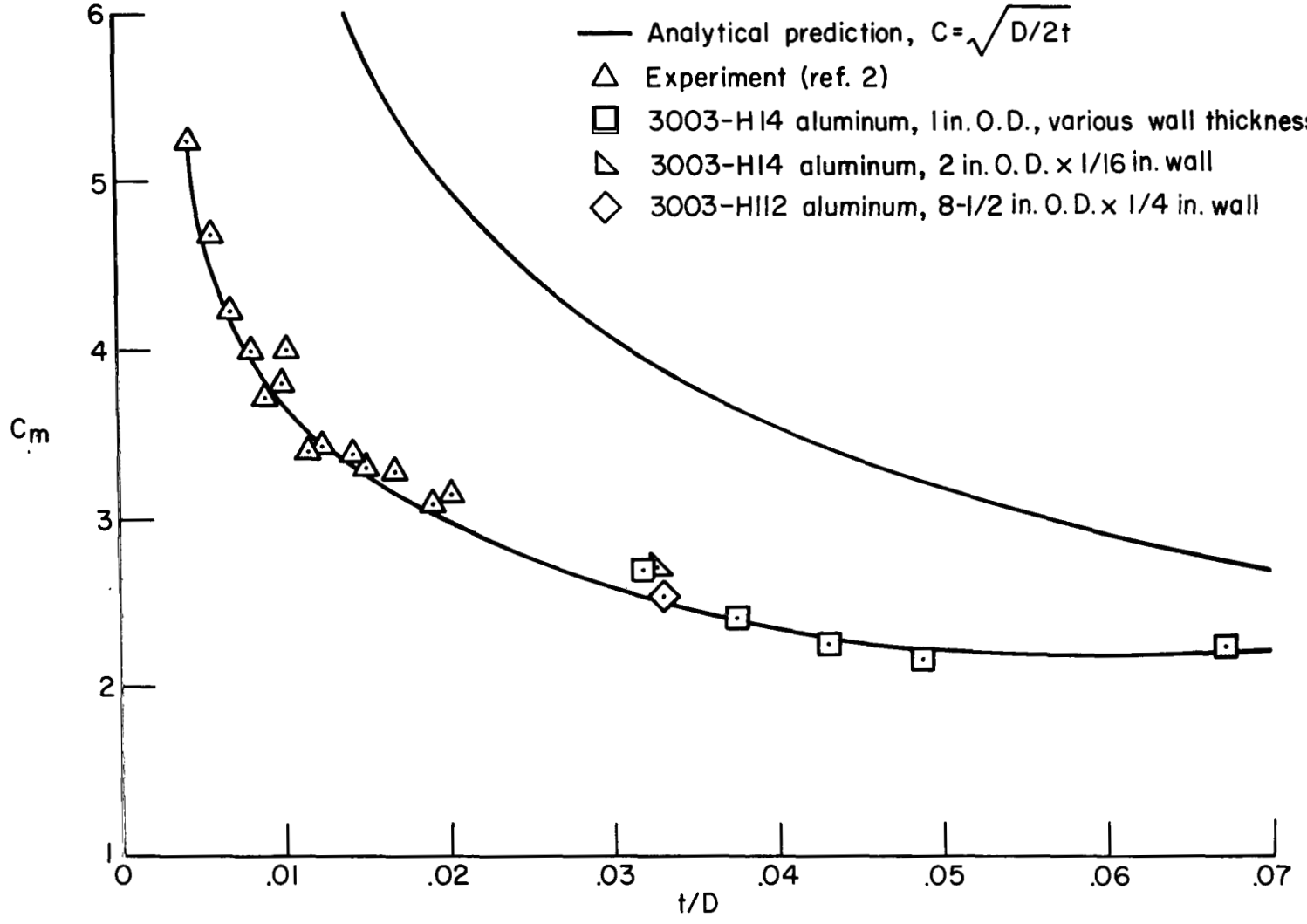

Figure 4.- Variation of equilibrium curvature parameter, C_m.

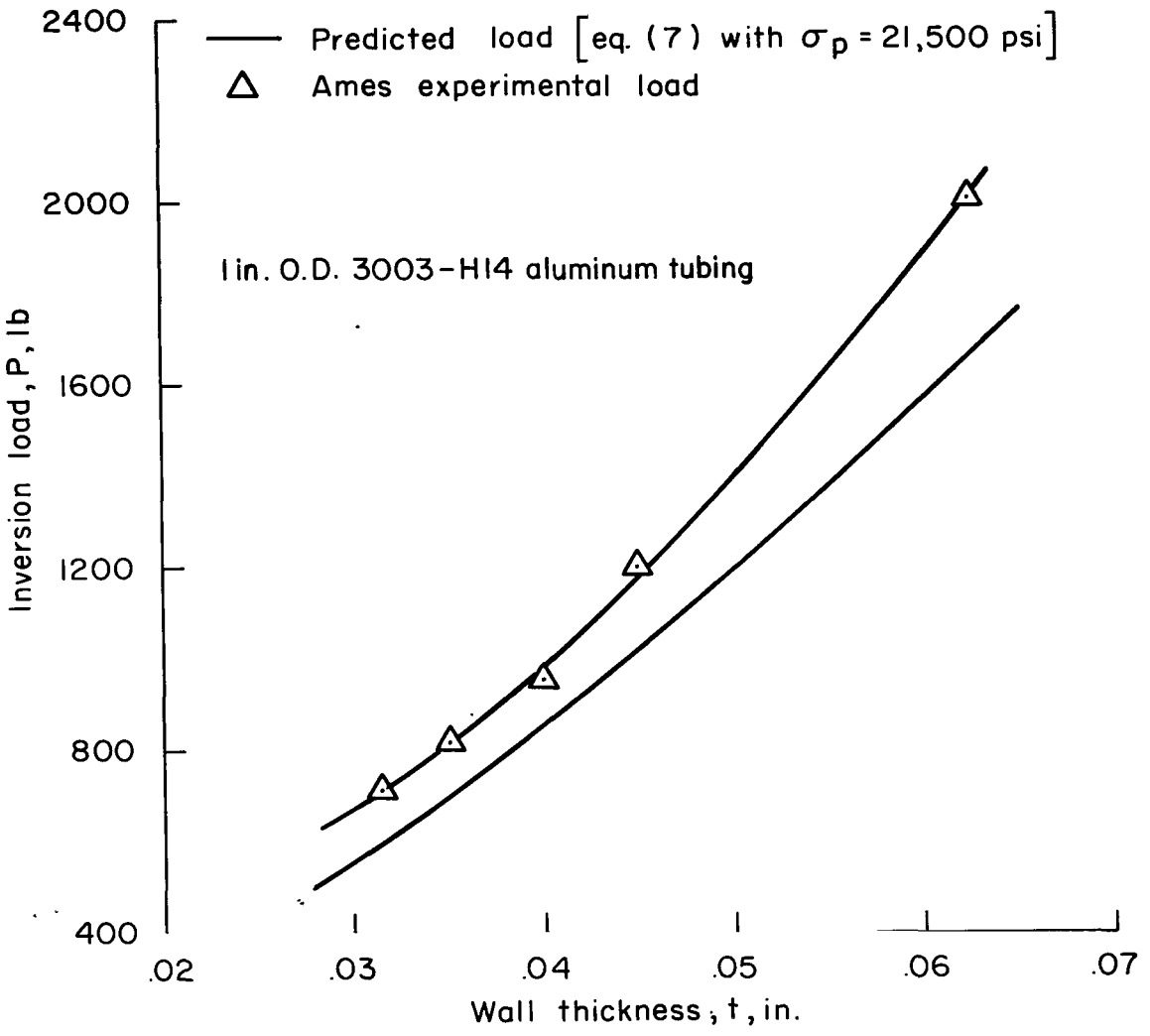

Figure 5.- Comparison of predicted and experimental inversion loads.

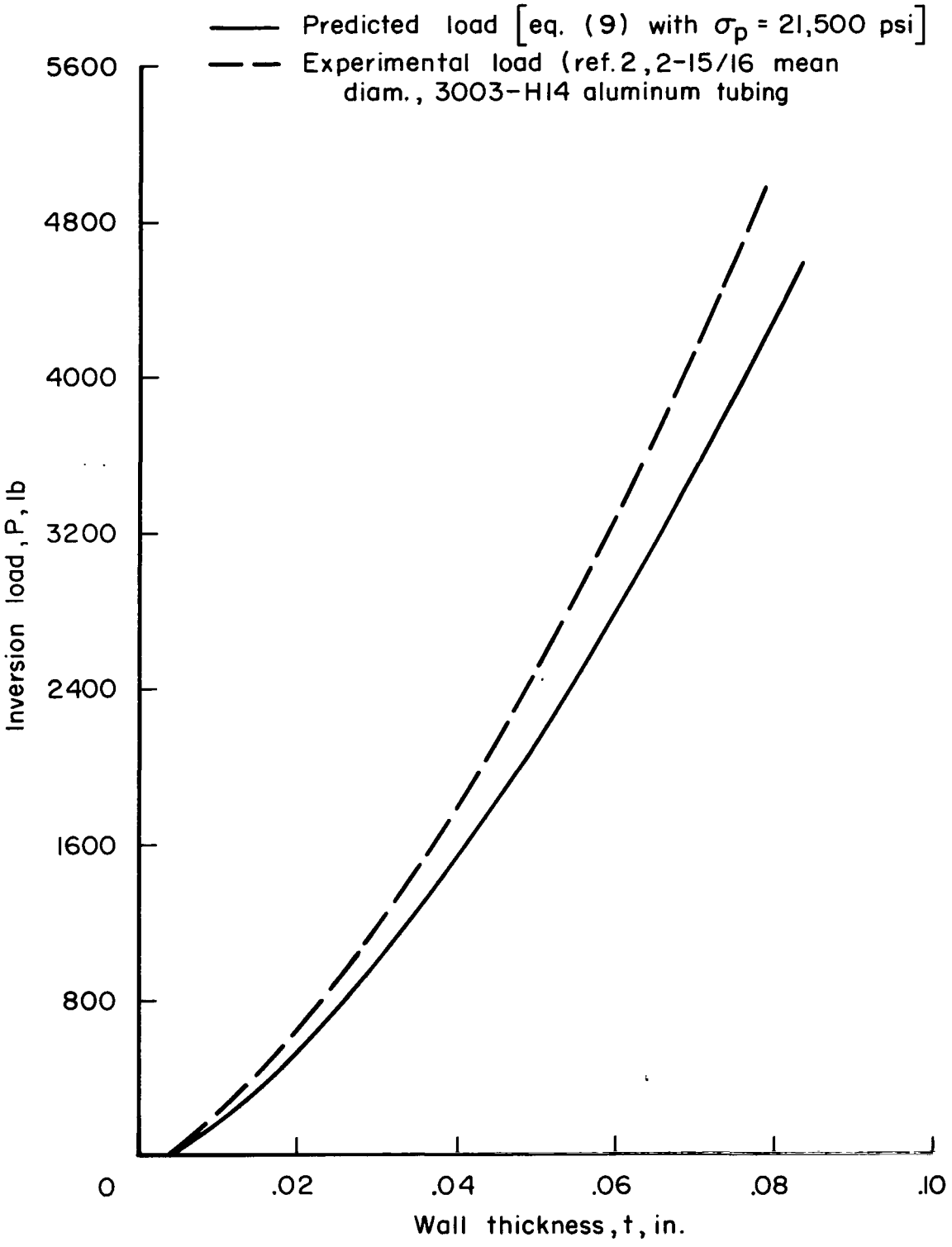

Figure 6.- Comparison of predicted and experimental inversion loads.

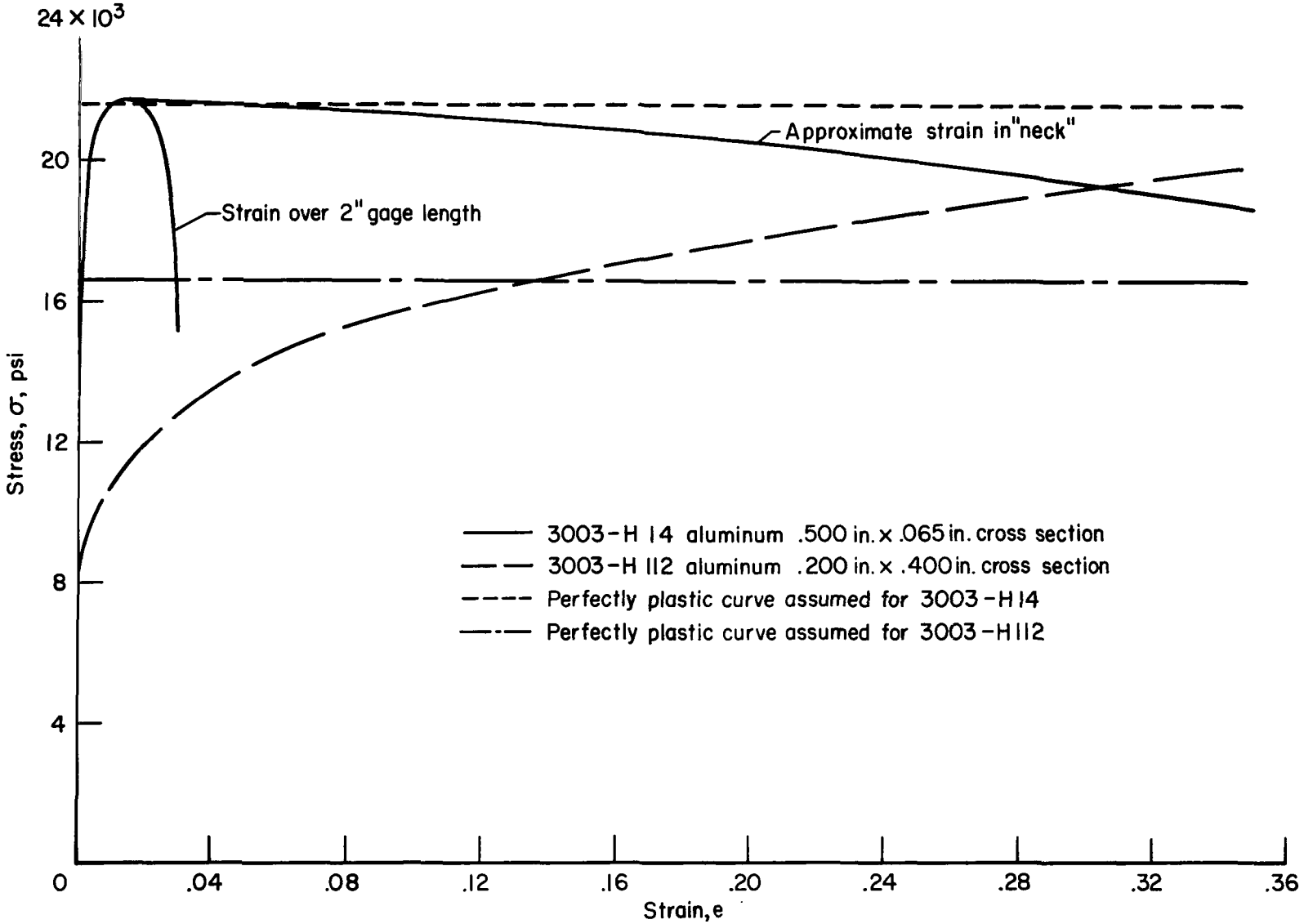

Figure 7.- Stress strain curves of 3003-H14 aluminum.

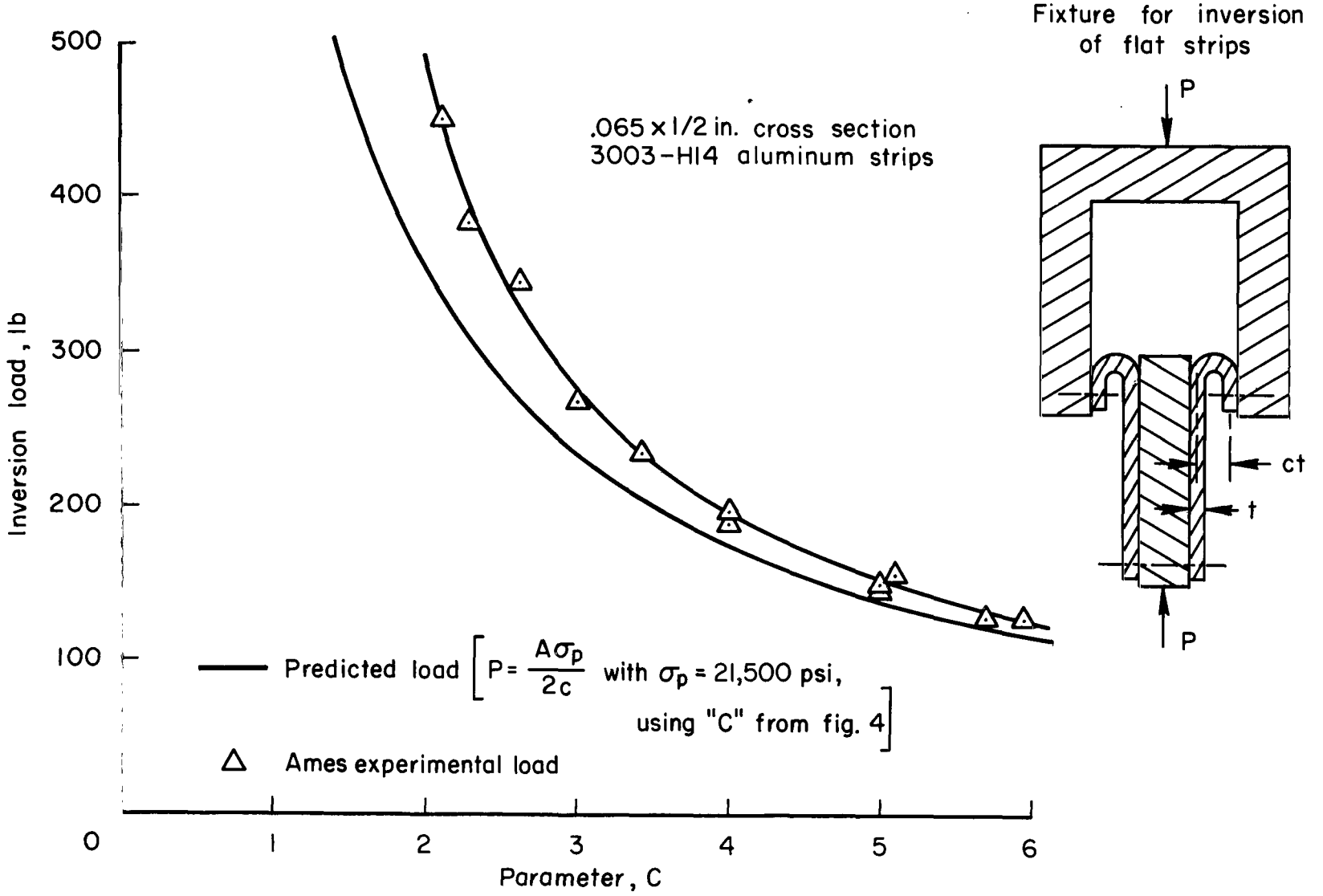

Figure 8.- Inversion of flat strips.

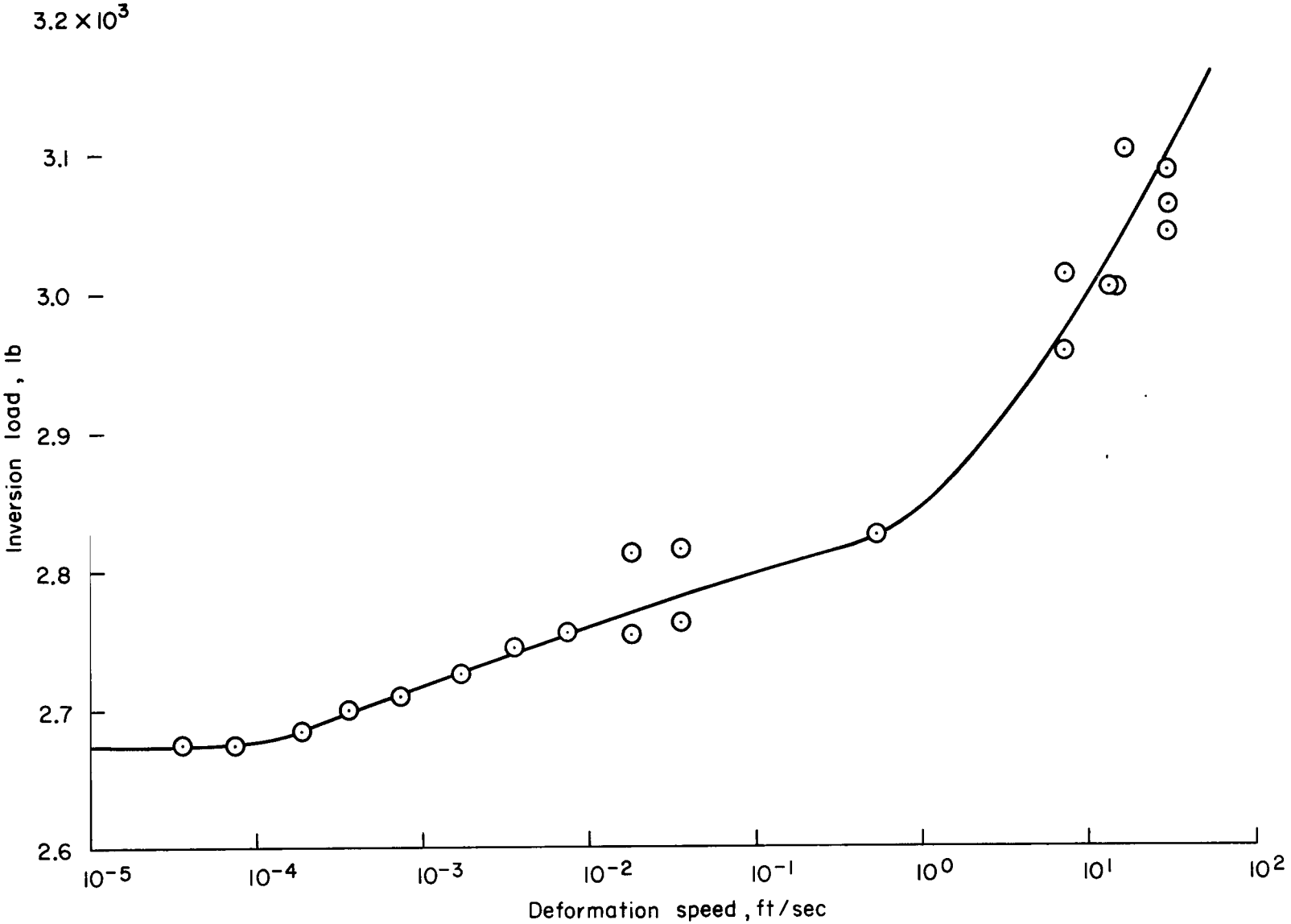

Figure 9.- Effect of deformation rate.

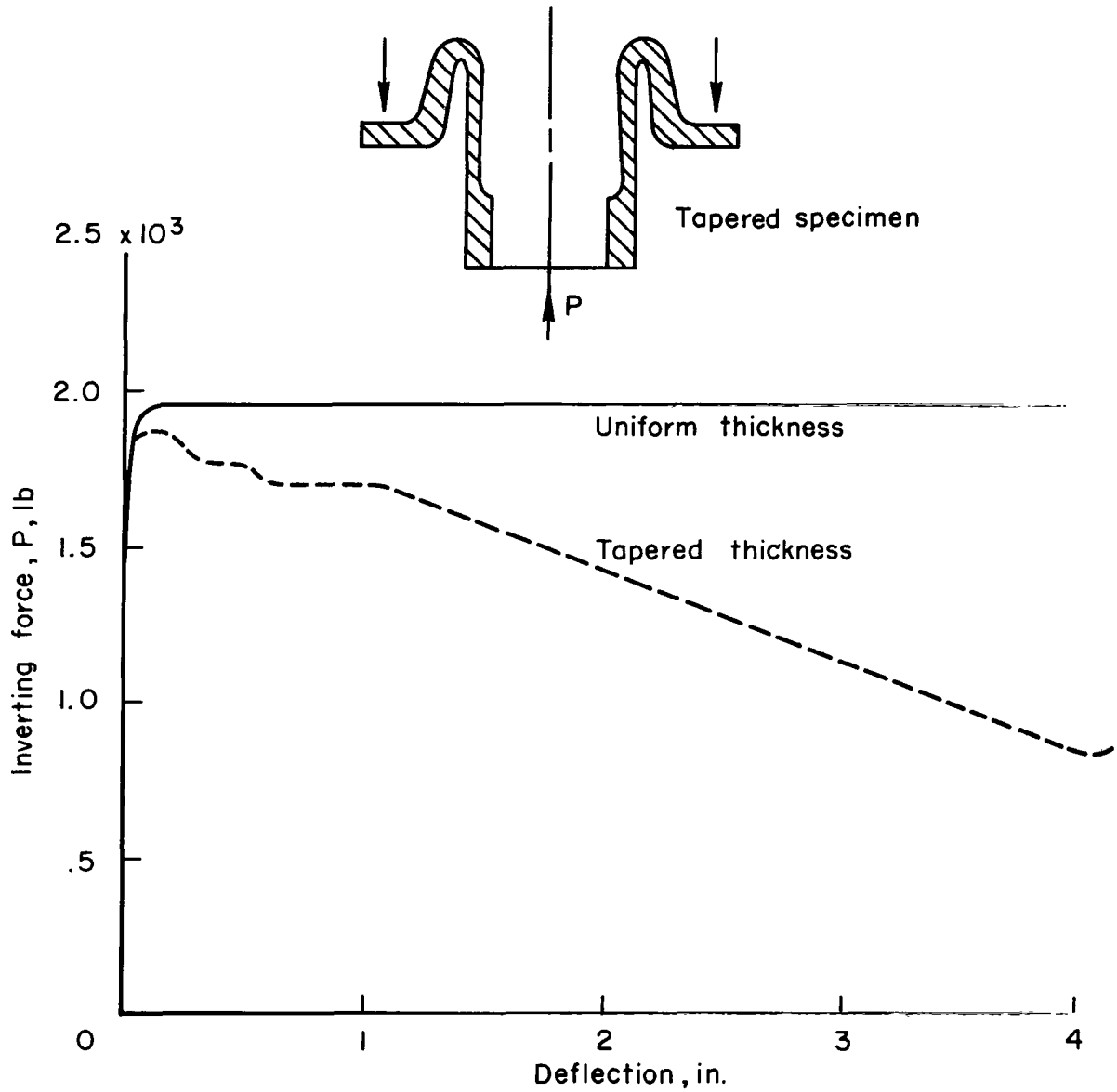

Figure 10.- Force versus deflection.

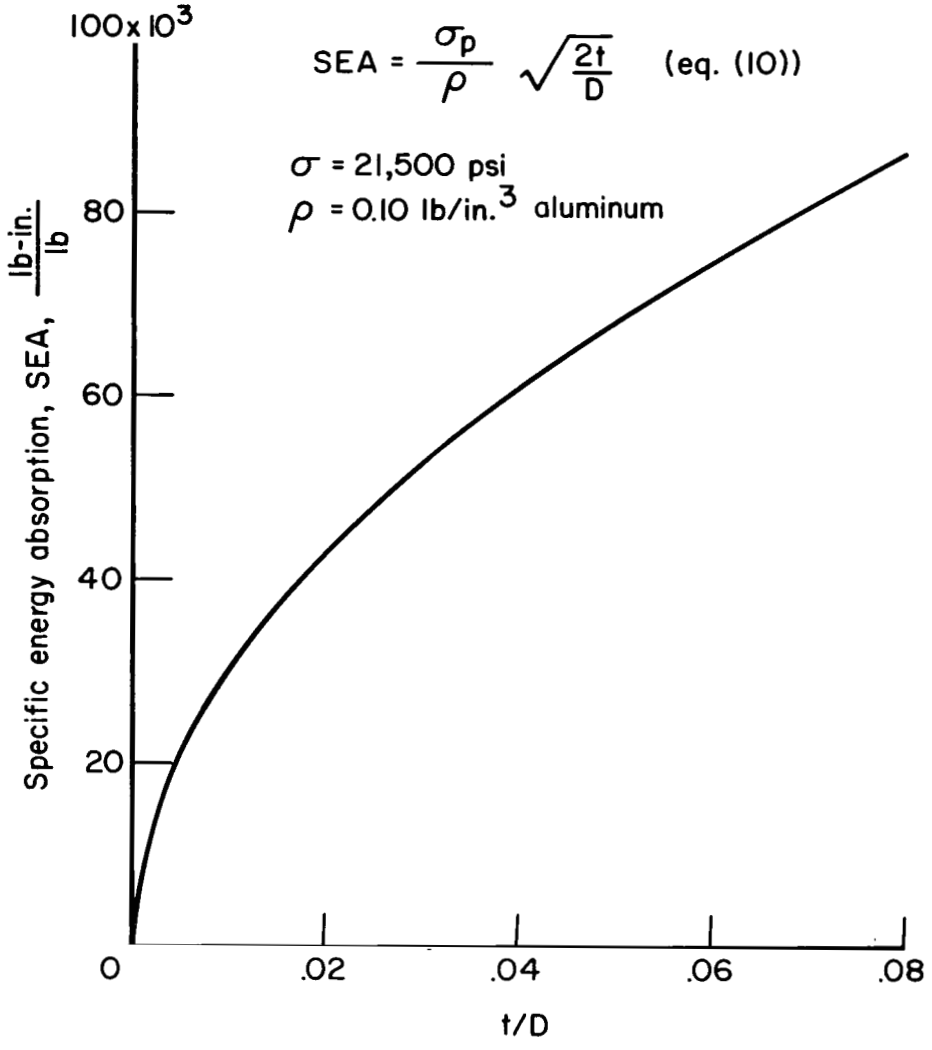

Figure 11.- Energy absorption efficiency.

"The aeronautical and space activities of the United States shall be conducted so as to contribute . . . to the expansion of human knowledge of phenomena in the atmosphere and space. The Administration shall provide for the widest practicable and appropriate dissemination of information concerning its activities and the results thereof."

—NATIONAL AERONAUTICS AND SPACE ACT OF 1958

NASA SCIENTIFIC AND TECHNICAL PUBLICATIONS

TECHNICAL REPORTS: Scientific and technical information considered important, complete, and a lasting contribution to existing knowledge.

TECHNICAL NOTES: Information less broad in scope but nevertheless of importance as a contribution to existing knowledge.

TECHNICAL MEMORANDUMS: Information receiving limited distribution because of preliminary data, security classification, or other reasons.

CONTRACTOR REPORTS: Technical information generated in connection with a NASA contract or grant and released under NASA auspices.

TECHNICAL TRANSLATIONS: Information published in a foreign language considered to merit NASA distribution in English.

TECHNICAL REPRINTS: Information derived from NASA activities and initially published in the form of journal articles.

SPECIAL PUBLICATIONS: Information derived from or of value to NASA activities but not necessarily reporting the results of individual NASA-programmed scientific efforts. Publications include conference proceedings, monographs, data compilations, handbooks, sourcebooks, and special bibliographies.

Details on the availability of these publications may be obtained from:

SCIENTIFIC AND TECHNICAL INFORMATION DIVISION

NATIONAL AERONAUTICS AND SPACE ADMINISTRATION

Washington, D.C. 20546